

SYNTHESIS AND CHARACTERIZATION OF ZINC SULPHIDE QUANTUM DOTS

Aye Mya Phyu¹, Yi Yi Myint²

Abstract

Zinc sulphide quantum dots (QDs) have been synthesized by the hydrothermal method. In this method, zinc acetate $Zn(CH_3CO_2)_2$ and sodium sulphide nonahydrate $Na_2S \cdot 9H_2O$ were used as starting materials. Glacial acetic acid was used to adjust the selected pH values of the system (pH=4, 5, and 6), and ammonia solution was used to obtain the pH values of the system (pH=8, 9, and 10). The synthesized ZnS QDs were characterized by using X-ray Diffraction Analysis (XRD), Fourier Transform Infrared Spectroscopy (FT IR), and UV-Visible Spectroscopy. The crystallite size range (8-13 nm) of the synthesized ZnS QDS was determined from the results of the XRD patterns by using Debye-Scherrer's equation. From the FT IR spectrum, a metal-sulphur bond (Zn-S) was found at 639 cm^{-1} . UV/Vis spectra indicated the absorption wavelengths of ZnS QDs at 270 nm.

Keywords: Quantum dots, hydrothermal method, zinc sulphide, Debye-Scherrer's equation

Introduction

Quantum dots are small, fluorescent nanocrystals that are $< 10\text{ nm}$ in diameter (Suri *et al.*, 2013). Quantum dots are generally constructed from elements of Groups II (e.g., Zn, Cd), -IV (e.g., Se, S), III-V, and IV-VI of the periodic table (Pawar *et al.*, 2018). Quantum dots are semiconductor nanocrystals resistant to chemical degradation, high thermal stability, and optical properties (high brightness) (Grigore *et al.*, 2017). Semiconductor nanocrystals of ZnS have been extensively studied for their quantum confinement effect, dielectric confinement effect, and unique size-dependent photoemission properties (Jothi *et al.*, 2013). ZnS nanoparticles have attracted great interest because of their potential applications in field effect transistors, light emitting diodes, photocatalysis, solar cells, and biological sensors (Xue *et al.*, 2011). The semiconducting quantum dots (QDs) have full access to the whole solar spectrum (Baruach *et al.*, 2019). For ZnS nanoparticles, the band gap increases with the decrease in particle size, which results in a blue shift of the absorption onset (Xue *et al.*, 2011). Hydrothermal methods have been reported for the synthesis of QDS with small crystal size, a narrow distribution, good crystallinity, and high photoluminescence intensity (Bodo and Singha, 2016).

ZnS is highly suitable as a window layer in hetero-junction photovoltaic solar cells because the wide band gap decreases the window absorption loss and improves the short circuit current of the cell (Jothi *et al.*, 2013). ZnS is a polymorphous material that exists in two crystalline forms, namely zinc blend (sphalerite) and Wurtzite. In both forms, the co-ordination geometry is at the Zn and S tetrahedrals. Zinc blend has a more stable cubic form (fcc), whereas wurtzite has a hexagonal form (hcp). ZnS exhibits a large band gap of approximately 3.54 eV and 3.91 eV for zinc blend and wurtzite, respectively. Zinc blend has four asymmetric units in its unit cell, where wurtzite has 2. Nano ZnS possess anomalous physical and chemical properties such as an enhanced surface to volume ratio, the quantum size effect, the surface to volume effect, the macroscopic quantum tunnelling effect, more optical absorption, chemical activity and thermal resistance, catalysis, and a low melting point (Kaur *et al.*, 2016).

¹ Department of Chemistry, Meiktila University

² Department of Educational Research, Planning and Training, Yangon

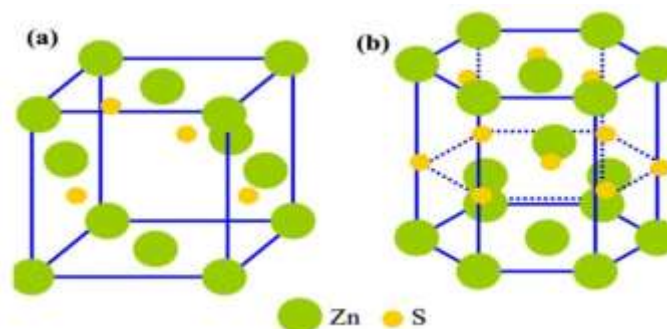


Figure 1. Crystalline structure of ZnS (a) cubic sphalerite and (b) hexagonal wurtzite (Kaur *et al.*, 2016)

Materials and Methods

Preparation of Zinc Sulphide Quantum Dots (ZnSQDs) by Hydrothermal Method

Firstly, 0.22 g of zinc acetate was dissolved in 120 mL of distilled water to get solution A. 0.4 g of sodium sulphide nonahydrate was dissolved in 20 mL of distilled water to obtain solution B. Solution A and solution B were mixed. Then glacial acetic acid solution was used to adjust the selected pH values of the system (pH = 4, 5, 6), and ammonia solution was used to obtain the pH values of the system (pH = 8, 9, 10).

The resultant solution was sonicated in the ultrasonic bath for 30 minutes. After sonication, the solution was transferred into a Teflon vessel, and then the vessel was put into a stainless steel tank to perform the hydrothermal treatment, which was placed in a vacuum oven at 140 °C for 24 h. Then it was cooled to room temperature. After cooling, the collected precipitates were washed several times with distilled water and ethanol until a neutral solution was obtained. And then it was allowed to stand for precipitation. The precipitates obtained were poured into the Petri dish and dried at room temperature for three days. Then the dried powder was placed in crucibles, and it was carried out under vacuum at 50 °C for 10 h.

In this way, 0.10410 g of dried sample (ZnS 8) of pH 8, 0.1145 g of dried sample (ZnS 9) of pH 9, 0.12183 g of dried sample (ZnS 10) of pH 10, 0.11028 g of dried sample (ZnS 4) of pH 4, 0.08351 g of dried sample (ZnS 5) of pH 5, and 0.11620 g of dried sample (ZnS 6) of pH 6 were obtained. The dried samples were used for further characterization.

Characterization of Prepared Zinc Sulphide Quantum Dots Powder by XRD, FT IR, and UV-Visible Analysis

XRD analysis

Powder x-ray diffraction (XRD) patterns were obtained by using a Rigaku Multiplex 2 kW, x-ray diffractometer with Cu-K α radiation of wavelength 1.54056 Å.

FT IR analysis

The sample using (1% KBr) was first inserted separately in the sample holder (cassette). The KBr sample was then pressed into solid discs. Then, using air as a reference, each pellet was analyzed using a Perkin Elmer 1600 Fourier Transform Infrared Spectrometer (FT-IR) with a scan speed of 16 scans/sec from 400 to 4000 cm $^{-1}$. It was used to identify the functional groups present in the sample.

UV-Visible analysis

The samples were examined by a UV-Visible spectrophotometer for the absorption spectrum (λ_{\max}).

Results and Discussion

Yield percent of ZnS quantum dots

Table 1 shows the yield percents of the prepared zinc sulphide quantum dots. The percent yield was calculated by using the formula,

$$\text{Yield (\%)} = \frac{\text{Actual Yield}}{\text{Theoretical Yield}} \times 100$$

Higher yield percentages were obtained at higher pH values. In this study, the highest yield percent of 99 was obtained using pH 10.

Table 1. Percent Yield of Zinc Sulphide Quantum Dots (Based on amount of zinc acetate)

No.	Nanoparticle (QDs)	Yield (%)
1	ZnS 4	85 %
2	ZnS 5	68 %
3	ZnS 6	85 %
4	ZnS 8	85 %
5	ZnS 9	85 %
6	ZnS 10	99 %

X-ray analysis

From X-ray analysis, XRD patterns and their respective data for ZnS quantum dots are shown in Figure 2 and Table 2 for ZnS 4, Figure 3 and Table 3 for ZnS 5, Figure 4 and Table 4 for ZnS 6, Figure 5 and Table 5 for ZnS 8, Figure 6 and Table 6 for ZnS 9, and Figure 7 and Table 7 for ZnS 10.

In each XRD pattern, the most intense peak was found along the plane (111), with the d-spacing about 3.16 Å at a 2θ value of 28° , indicating the orientation of the majority of the nanocrystallites along this axis. Other prominent peaks were found for the plane (220), with the d-spacing 1.92 Å at a 2θ value of 47° and the plane (311), with the d-spacing 1.64 Å at a 2θ value of 56° . All the peaks are well matched with the standard peaks from the library. It is also noticed that there are either no extra or any impurity phases evident in ZnS samples, indicating that the prepared samples are single-phase with high purity.

The broadened peaks indicated the smaller particle size of the sample. The average crystallite sizes of the quantum dots are calculated by Debye Scherrer's formula, $D = \frac{K\lambda}{\beta \cos \theta}$, where

D is the average crystallite size in nm, K is proportionally constant, λ is the wavelength of incident x ray (1.54056 Å), β is the full width at half maximum (FWHM), and θ is the Bragg angle. The average crystallite sizes were calculated to be 8.65 nm for ZnS 4, 8.30 nm for ZnS 5, 7.9 nm for ZnS 6, 9.10 nm for ZnS 8, 8.30 nm for ZnS 9, and 12.40 nm for ZnS 10.

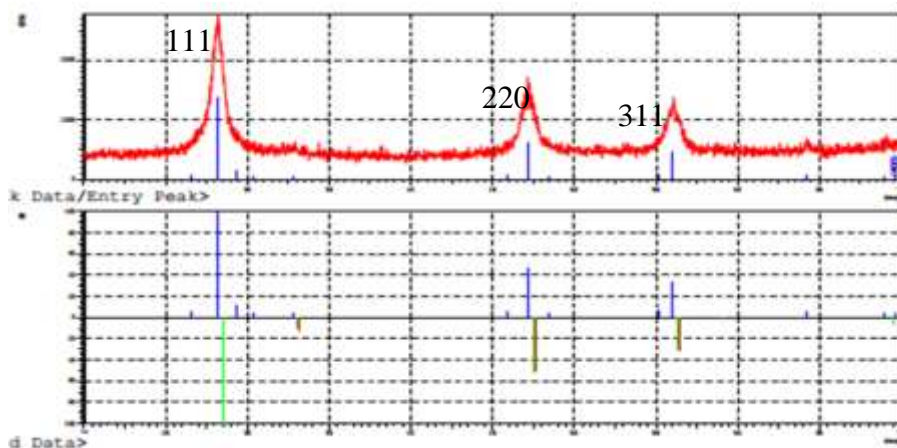


Figure 2. XRD diffraction pattern of prepared ZnS 4

Table 2. X-ray Diffraction Peaks Data of Prepared ZnS 4

No.	2θ ($^{\circ}$)	d (\AA)	FWHM ($^{\circ}$)	Crystallite size (\AA)	Crystallite size (nm)	Miller indices (h k l)
1	28.1826	3.16387	0.90360	90.6	9.06	111
2	47.1609	1.92558	1.04930	82.5	8.25	220
3	56.0257	1.64009	1.04000	86.4	8.64	311

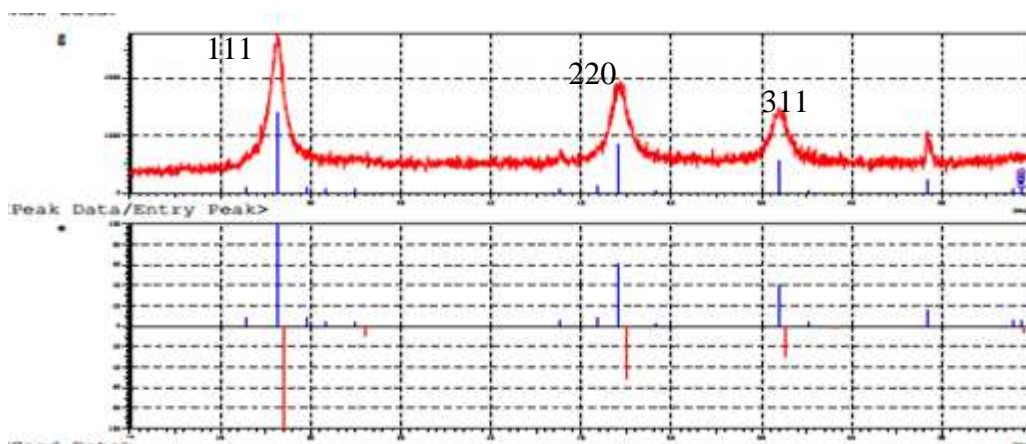


Figure 3. X-ray diffraction pattern of prepared ZnS 5

Table 3. X-ray Diffraction Peaks Data of Prepared ZnS 5

No.	2θ ($^{\circ}$)	d (\AA)	FWHM ($^{\circ}$)	Crystallite size (\AA)	Crystallite size (nm)	Miller indices (h k l)
1	28.1528	3.16715	0.96600	84.7	8.47	111
2	47.1163	1.92729	1.08000	80.0	8.00	220
3	55.9533	1.64204	1.06500	84.4	8.44	311

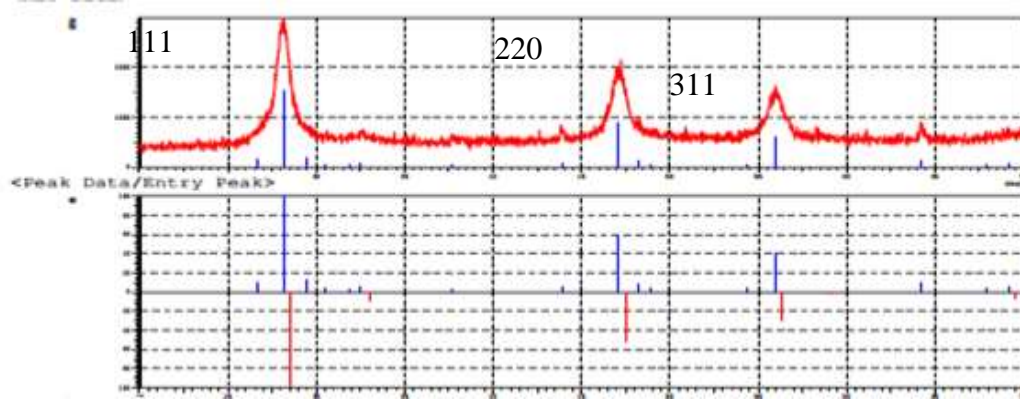


Figure 4. X-ray diffraction pattern of prepared ZnS 6

Table 4. X-ray Diffraction Peaks Data of Prepared ZnS 6

No.	2θ (°)	d (Å)	FWHM (°)	Crystallite size (Å)	Crystallite size (nm)	Miller indices (h k l)
1	28.1351	3.16910	0.95350	85.8	8.58	111
2	47.0996	1.92794	1.02000	69.7	6.97	220
3	47.0996	1.64177	1.06500	84.4	8.44	311

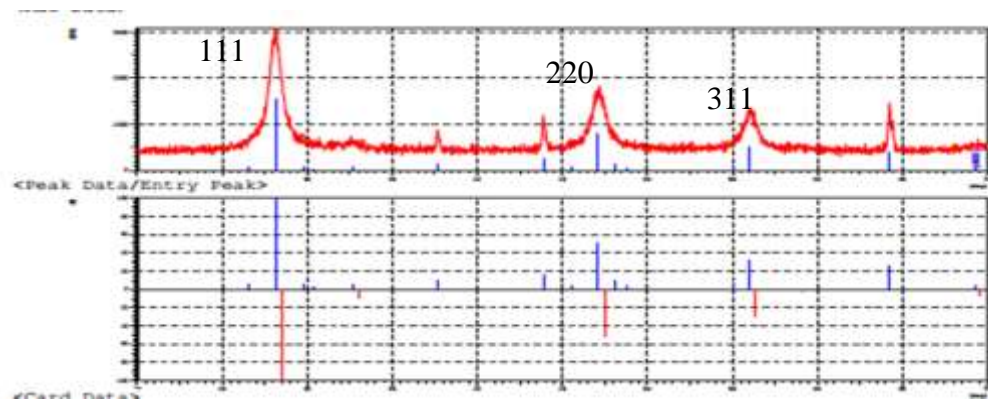


Figure 5. X-ray diffraction pattern of prepared ZnS 8

Table 5. X-ray Diffraction Peaks Data of Prepared ZnS 8

No.	2θ (°)	d (Å)	FWHM (°)	Crystallite size (Å)	Crystallite size (nm)	Miller indices (h k l)
1	28.1411	3.16844	0.90460	90.50	9.05	111
2	47.1196	1.92717	0.99000	87.50	8.75	220
3	56.0123	1.64045	0.94670	95.01	9.50	311

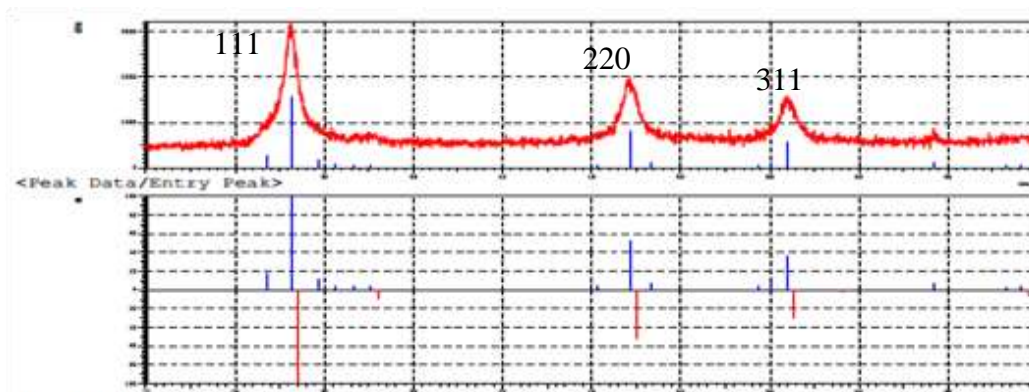


Figure 6. X-ray diffraction pattern of prepared ZnS 9

Table 6. X-ray Diffraction Peaks Data of Prepared ZnS 9

No.	2θ ($^{\circ}$)	d (\AA)	FWHM ($^{\circ}$)	Crystallite size (\AA)	Crystallite size (nm)	Miller indices (h k l)
1	28.1302	3.16964	1.00280	81.6	8.16	111
2	47.1296	1.92678	1.08000	80.1	8.01	220
3	55.9883	1.64110	1.02500	87.7	8.77	311

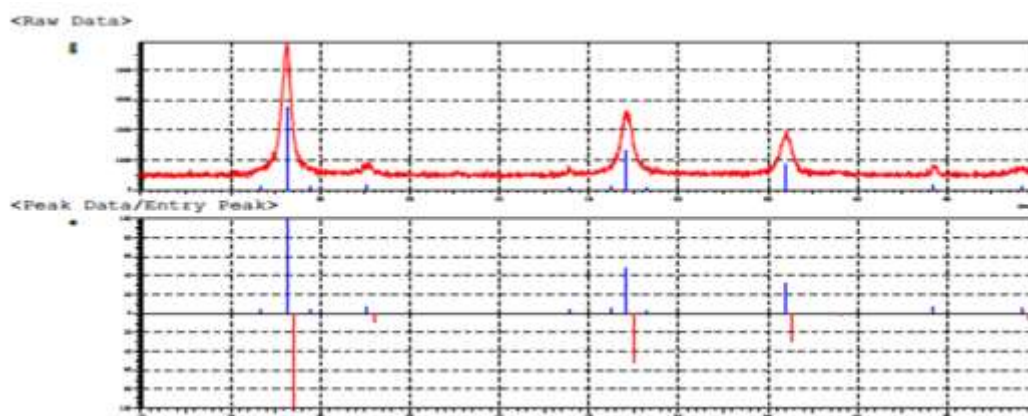


Figure 7. XRD diffraction pattern of prepared ZnS 10

Table 7. X-ray XRD Diffraction Peaks Data of Prepared ZnS 10

No.	2θ ($^{\circ}$)	d (\AA)	FWHM ($^{\circ}$)	Crystallite size (\AA)	Crystallite size (nm)	Miller indices (h k l)
1	28.1215	3.17060	0.61610	132.8	13.28	111
2	47.1024	1.92783	0.73430	117.9	11.79	220
3	55.9760	1.64143	0.73460	122.4	12.24	311

According to Table 8, the axial lengths a , b , and c are equal, and the angles, α , β and γ are 90° . Therefore, the crystalline structure of the synthesized zinc sulphide quantum dots is cubic. Since Miller indices are all odd and all even, it is face-centred cubic (fcc). The XRD results of the synthesized zinc sulphide quantum dots are consistent with the crystallite size and structure of zinc sulphide quantum dots.

Table 8. Lattice Parameters of Zinc Sulphide Quantum Dots for All Selected pH(s)

Phase name	a, Å	b, Å	c, Å	α , °	β , °	γ , °
Zinc sulphide	5.40600	5.40600	5.400600	90.000	90.000	90.000

FT IR analysis

FTIR is an analytical technique used to identify information about the chemical bonding in a material. The infrared absorption spectra (FTIR) of the ZnS quantum dots were recorded in the range of 400–4000 cm^{-1} , and the spectra are shown in Figures 8, 9, 10, and 11 with the spectral data described in Table 9. Spectrum analysis of the ZnS shows the presence of a broad and intense band at around 3330 cm^{-1} , which is attributed to the O-H stretching vibration (Silverstein *et al.*, 2005). The presence of a band around 1627 cm^{-1} may correspond to the O–H bending vibration. The presence of these bands indicates the existence of water on the surface of ZnS samples. The absorption at 1086 cm^{-1} indicates the C-O stretching vibration. The prominent peak at 639 cm^{-1} indicates the Zn-S (metal-sulphur bond) (Zhao *et al.*, 2007). The strong absorption bands in the range of 450–650 cm^{-1} are related to the vibrational characteristics of ZnS (Liu *et al.*, 2017).



Figure 8. FT IR spectrum of prepared ZnS 4

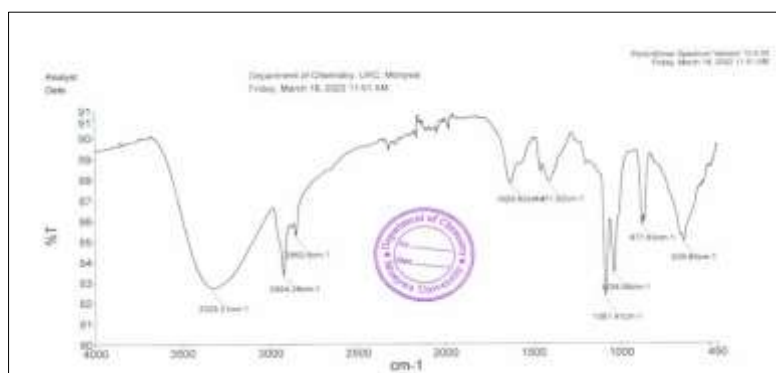


Figure 9. FT IR spectrum of prepared ZnS 5

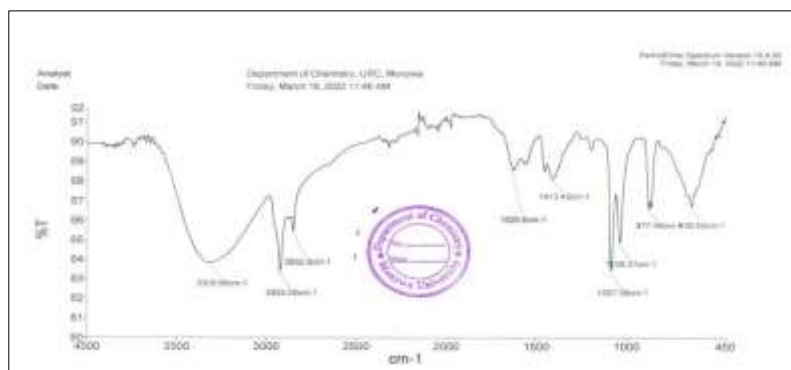


Figure 10. FT IR spectrum of prepared ZnS 6

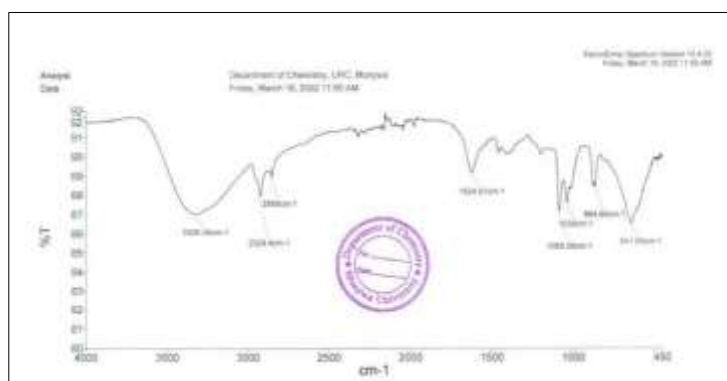


Figure 11. FT IR spectrum of prepared ZnS 9

Table 9. FT IR Assignments of Prepared ZnS Quantum Dots

	Observed frequency(cm^{-1})				Assignment	Literature frequency(cm^{-1})*
	ZnO 4	ZnO 5	ZnO 6	ZnO 9		
1	3334	3328	3308	3326	-OH stretching vibration	3550-3200
2	1627	1629	1629	1624	-OH bending vibration	1666-1586
3	1086	1087	1087	1085	C-O stretching vibration	1200-1000
4	639	639	639	639	Zn-S metal sulphide band	650-450

*Silverstein *et al.*, 2005; Frost *et al.*, 2002; Liu *et al.*, 2017

UV-visible analysis

The optical properties of ZnS quantum dots were determined from absorption measurements in the range of 200-600 nm. The absorption corresponds to electron excitation from the valence band to the conduction band. The plots of optical absorbance versus wavelength for prepared ZnS quantum dots are shown in Figures 12, 13, 14, 15, 16, and 17 for ZnS 4, ZnS 5, ZnS 6, ZnS 8, ZnS 9, and ZnS 10, respectively. In each absorption spectrum, the strongest absorption peak of the prepared ZnS sample appears at around 270 nm. UV/ Vis spectra indicate the absorption

wavelengths of ZnS 4, ZnS 5, ZnS 6, ZnS 8, and ZnS 10 are the same at 270 nm, and ZnS 9 is 260 nm. ZnS has good absorption for light in the wavelength range of 220-350 nm (Gadalla *et al.*, 2018).

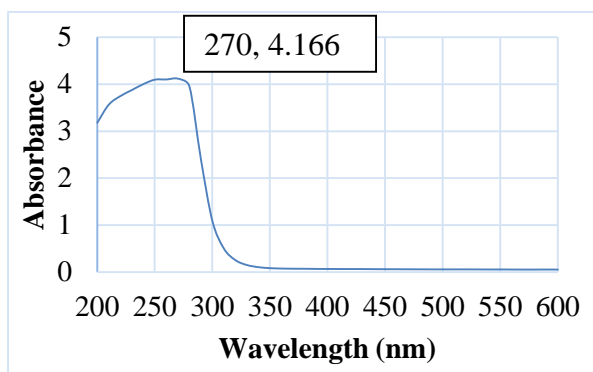


Figure 12. UV-visible spectrum of ZnS 4

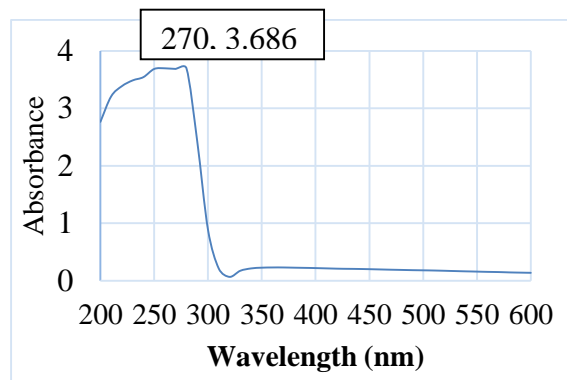


Figure 13. UV-visible spectrum of ZnS 5

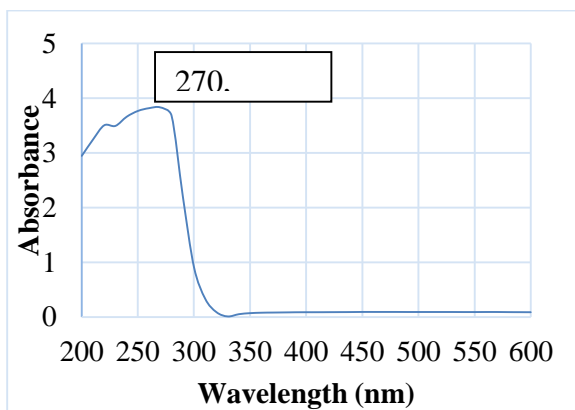


Figure 14. UV-visible spectrum of ZnS 6

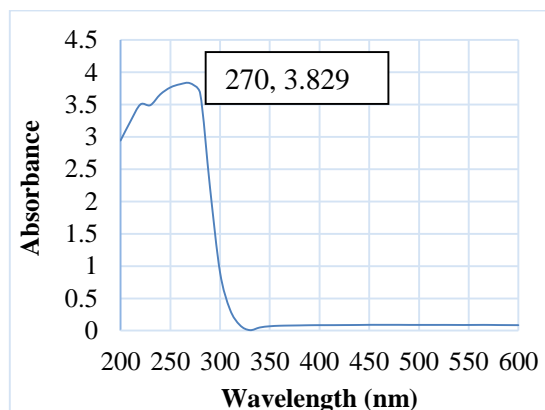


Figure 15. UV-visible spectrum of ZnS 8

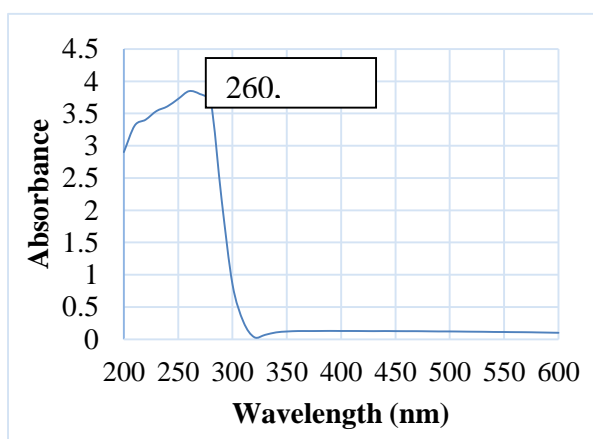


Figure 16. UV-visible spectrum of ZnS 9

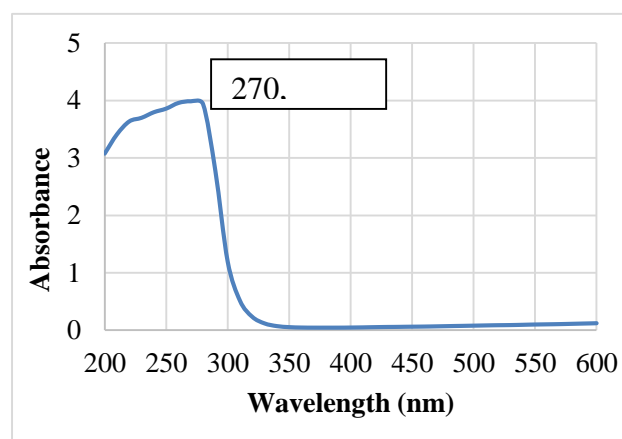


Figure 17. UV-visible spectrum of ZnS 10

Conclusion

In this research work, zinc sulphide quantum dots were synthesized by the hydrothermal method using zinc acetate and sodium sulphide nonahydrate as starting materials. The yield percents were found to be 68% of ZnS 5, 85 % of ZnS 4, Zn 6, ZnS 8, ZnS 9, and 99 % of ZnS 10 based on zinc acetate. By X-Ray Diffraction (XRD) analysis, zinc sulphide quantum dots were indexed as face-centred cubic, and the average crystallite sizes were observed in the range

of 7.9 to 12.4 nm. FT IR spectra of all zinc sulphide quantum dots showed a strong peak at 639 cm^{-1} . UV/Vis spectra indicated the absorption wavelengths of ZnS 4, ZnS 5, ZnS 6, ZnS 8, and ZnS 10 were the same at 270 nm, and ZnS 9 was at 260 nm. In an acidic medium, the higher the pH values, the smaller the crystallite sizes observed. So as to regard all the pH values used in acidic conditions, the crystallite sizes are inclusive of quantum dot sizes. In an alkaline medium, the crystallite size at pH 10 deviates from quantum dot sizes.

Acknowledgements

The authors would like to thank the Department of Higher Education, Ministry of Education, Yangon, Myanmar, for allowing us to carry out this research programme. Thanks are also extended to the Myanmar Academy of Arts and Science and Professor Dr Thandar Aung, Head of the Department of Chemistry, Meiktila University, for allowing us to carry out this research programme.

References

- Baruah, J. M., S. Kalita, and J. Narayan. (2019). "Green Chemistry Synthesis of Biocompatible ZnS Quantum Dots (QDs): Their Application as Potential Thin Films and Antibacterial Agent". *International Nano Letters*, vol.9, pp.149-159
- Bodo, B., and R. Singha. (2016). "Structural and Optical Properties of ZnS Quantum Dots Synthesized by CBD Method". *International Journal of Scientific and Research Publications*, vol. 6 (8), pp.461-465
- Frost, R.L., P.A. Williams, W. Martens, and T. Kloprogge. (2002). "Raman and Infrared Spectroscopic Study of the Vivianite-group Phosphates Vivianite, Baricite and Bobierrite". *Mineralogical Magazine*, vol. 66 (6), pp.1063-1073
- Gadalla, A., M.S. Abd el-Sadekb, and R. Hamood. (2018). "Synthesis, Structural and Optical Characterization of CdS and ZnS Quantum Dots". *Chalcogenide Letters*, vol. 15 (5), pp. 281 - 291
- Grigore, M. E., A.M. Holban, and A. M. Grumezescu. (2017). *Nanotherapeutics in the Management of Infections and Cancer*. In Nanobiomaterials Science, Development and Evaluation. Razavi, M., and A. Thakor (Editors). Amsterdam: Elsevier, pp.163-189
- Jothi, N.S.N, A.G. Joshi, R.J. Vijay, A. Muthuvinnayagam, and P. Sagayaraj. (2013). "Investigation on One-pot Hydrothermal Synthesis, Structural and Optical Properties of ZnS Quantum Dots". *Materials Chemistry and Physics*, vol. 138, pp.186-191
- Kaur, N., S. Kaur, J. Singh and M. Rawat. (2016). "A Review on Zinc Sulphide Nanoparticles: From Synthesis, Properties to Applications". *Journal of Bioelectronics and Nanotechnology*, vol. 1(1), pp.1-5
- Liu, L.N., J.G. Dai, T.J. Zhao, S.Y. Guo, D.S. Hou, P. Zhang, J. Shang, S. Wang, and S. Han. (2017). "A Novel Zn(II) Dithiocarbamate/ZnS Nanocomposite for Highly Efficient Cr^{6+} Removal from Aqueous Solutions". *RSC Adv.* vol. 7, pp.35075-35085
- Pawar, R.S., P.G. Upadhaya, and V.B. Patravale. (2018). *Quantum Dots: Novel Realm in Biomedical and Pharmaceutical Industry*. In Handbook of Nanomaterials for Industrial Applications. C.M. Hussain (Editor). Amsterdam, Elsevier, pp.621-637
- Silverstein, R.M., F.X. Webster, and D.J. Kiemle. (2005). *Spectrometric Identification of Organic Compounds*. New York: 7th edition, John Wiley and Sons, pp.88-89
- Suri, S., G. Raun, J. Winter, and C. E. Schmidt. (2013). *Microparticles and Nanoparticles*. In Biomaterial Science. Ratner, B.D., A.S. Hoffman, F.G. Schoen, and J.E. Lemons (Editors). London: 3rd edition, Academic Press
- Xue, L., C. Shen, M. Zheng, H. Lu, N. Li, G. Ji, L. Pan and J. Cao. (2011). "Hydrothermal Synthesis of Graphene-ZnS Quantum Dot Nanocomposites". *Materials Letters*, vol. 65, pp. 198-200
- Zhao, Y., F. Wang, Q. Fu, W. Shi. (2007). "Synthesis and Characterization of ZnS/hyperbranched Polyester Nanocomposite and its Optical Properties". *Polymer*, vol.48, pp.2853-2859